Ryerson University

Department of Mechanical and Industrial Engineering

Faculty of Engineering and Architectural Science

Course Number	MEC 751
Section Number	03
Course Title	Measurements,Instruments &Sensors
Semester/Year	Fall 2019
Instructor	Dr. Ahmad Ghasempoor

Rack and Pinion Linear Control

Submission Date	Nov 25, 2019
Due Date	Nov 25, 2019

Name	Student ID	Signature
Sina Sartipzadeh Amirghasemi	01049	Sina
Ramish Syed	44299	
Chitransh Vishway	60402	
Syed Mehdi	50946	SM Wasi

*By signing above you attest that you have contributed to this submission and confirm that all work you have contributed to this submission is your own work. Any suspicion of copying or plagiarism in this work will result in an investigation of Academic Misconduct and may result in a "0" on the work, an "F" in the course, or possibly more severe penalties, as well as a Disciplinary Notice on your academic record under the Student Code of Academic Conduct, which can be found online at: http://www.ryerson.ca/senate/policies/pol60.pdf.

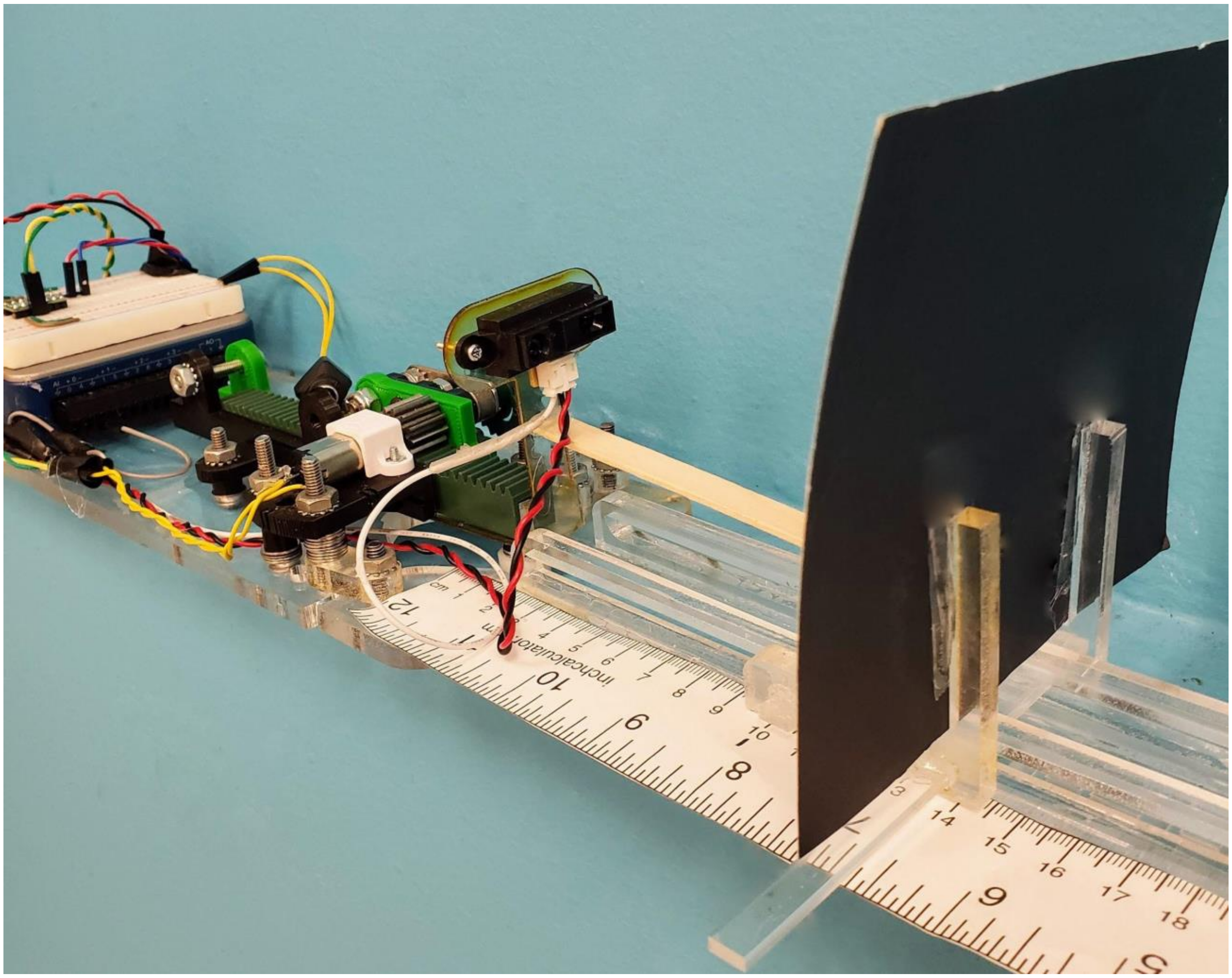

RACK AND PINION LINEAR MOTION CONTROL

Chitransh Vishway
Ramish Syed
Syed Mehdi
Sina Sartipzadeh Amirghasemi

Fall 2019
Measurements, Instruments & Sensors
Ryerson University

SUMMARY

The purpose of the rack and pinion linear tracker is to be able to emulate the autonomous movement of a linear fume tracker. It does so by using a Sharp IR sensor (Block A) to measure the distance between itself, and the user controlled secondary piece (Block B). The system works by receiving signals from the distance sensor, then relaying those values to LabVIEW; where it proceeds to calculate the position error and energizes the motor to translate the position of the rack. Block B had a range of ±5cm and was made of a black piece of paper glued onto a rail system. The micrometal gear motor has a torque of 260 μNm as specified by the manufacturer, and it was observed that only 76.1 μNm of torque was required to move the rack. The final results exhibited the following values for the various errors present in the calibration of the system. These errors were found based on the data collected from the calibration of the final design, all of which have a full scale of 3 V. The non-linearity error was found to be ±0.0045 V , which was 0.3% Full Scale Output (FSO). A zero offset error of ±0.265 V, being 17.67% of the FSO; the repeatability error was found to be ±0.005 V, being 0.33% of the FSO. Hysteresis error of ±0.01V being 0.66% of the FSO. The rise time of the dynamic response was found to be 17 ms**,** and a settling time of 8 ms. The system settles at approximately 10.01 cm at steady state. These values were collected using the LabVIEW VI, and in conjunction with excel, appropriate values were calculated and recorded. CAD drawings for the tracker are found in Appendix 2: Materials and CAD drawings, which were created using Solidworks.

TABLE OF CONTENTS

TABLE OF CONTENTS 3

1.0 INTRODUCTION 5

2.0 MECHANICAL SYSTEM 6

2.1 Initial Concepts 6

2.2 MECHANICAL DESIGN 9

3.0 ELECTRICAL SYSTEM AND DATA ACQUISITION 11

3.1 Model of Wiring 11

3.2 Sensor calibration 11

I. Static Calibration 11

II. Dynamic calibration 12

3.3 Signals 12

4.0 CONTROL SYSTEM 12

4.1 Labview Program Description 16

4.2 Sensor Sub VI 16

4.3 Motor Sub VI 18

5.0 Results & Evaluation 21

5.1 Static Calibration 21

I. Calibration results 21

II. Process of calibration 22

5.2 Noise and other sources of error 22

6.0 Discussion 25

7.0 Conclusion 26

8.0 References 27

9.0 Appendix

9.1 Appendix 1: Torque calculation of motor 28

9.2 Appendix 2: Materials and CAD Drawings 29

9.3 Appendix 3: Calibration Data from Milestone 2 35

9.4 Appendix 4: Final Calibration Data 36

9.5 Appendix 5: Static Error Calculation 37

List of Figures

Figure 1: System Interfaces…………………………………………………………………….6
Figure 2: Solidworks CAD Model of Rack & Pinion Design…………………………………….9
Figure 3: Sheared 3D printed side plate…………………………………………………………10
Figure 4: Rack and Pinion Shaft Keys………………………………………………………...10
Figure 5: Breadboard Wiring……………………………………………………………………11
Figure 6: Block Diagram of the Control System implementing PD Control……………………13
Figure 7: Flowchart of PD Control System……………………………………………...15
Figure 8: Sensor SubVI…………………………………………………………………….16
Figure 9: Flowchart of Sensor SubVI Operation………………………………………...17
Figure 10: Motor SubVI……………………………………………………………………18
Figure 11 Flowchart for Motor SubVI Operation………………………………………..19
Figure 12: Front Panel of Main Program………………………………………………..20
Figure 13: Sensitivity Equation………………………………………………………….21
Figure 14: Step Response of the System (Distance)……………………………………..23
Figure 15: Step Response of the System(Voltage)……………………………………....23
Figure 16: Rise time of System Response (Step Input 5 cm) ……………………………...24
Figure 17: Rise time of System Response (Step Input 5 cm)……………………………....25
Figure 18: Pinion connected to Motor……………………………………………………...28
Figure 19: Base Plate Acrylic……………………………………………………………….30
Figure 20: Side Plate Acrylic………………………………………………………………30
Figure 21: Rack Bottom Acrylic…………………………………………………………....31
Figure 22: Rack Hard Plastic……………………………………………………………….32
Figure 23: Pinion Cast Steel………………………………………………………………..33
Figure 24: Train Side Plate Acrylic………………………………………………………...33
Figure 25: Train Slider Acrylic……………………………………………………………..34
Figure 26: Train Base Acrylic……………………………………………………………….34
Figure 27: Main Plate Hard Plastic………………………………………………………….35

List of Tables

Table 1: Morphological Chart………………………………………………………………..7
Table 2: Signal Chart for Motor…………………...……………………………………….12
Table 3: Calibration Chart Voltage & %FSO(5V) ……………………………………....21
Table 4: Dynamic Calibration Results……………………………………………………...23
Table 5: List of Materials…………………………………………………………………...29
Table 6: Static Calibration & Error Results………………………………………………...36
Table 7: Dynamic Calibration Results……………………………………………………...36
Table 8: Final Calibration Data……………………………………………………………37
Table 9: Static Error Calculations …………………………………………………………38

1.0 INTRODUCTION

A linear fume tracker works by moving itself to and from the welding site, such that it keeps a close proximity to a work area where it can collect fumes that are created through welding of parts. It functions in this nature by reading a signal to keep the distance between itself and the welding gun at an optimal value.

The objective of the project is to be able to design an effective model which mimics this dynamic behavior of the sensor or control system to gain a greater understanding of how the full scale design process would take place. The prototype to model this behavior is to be designed such that an extractor hood (Block A) and welding gun (Block B). The prototype is intended to function by moving a certain distance, forwards and backwards and in doing so the follower, Block A will move towards Block B, and continuously maintain a distance of 10 cm. Block B had a range of ±5cm and was made of a black piece of paper glued onto a rail system[1].

The core parts to create the prototype model include the motor, motor driver chip, and utilized PWM Control for its function. The Micro Metal Gearmotor HP 6 V with Extended Motor Shaft, used in the prototype which uses a total gear ratio value, of 297.92:1 and is a high powered (HP) 6 V motor, which comes equipped with an extended motor shaft for a greater length for greater practical results.[2] The DRV8835 Dual Motor Driver Carrier, which when installed on a breadboard, coordinates with the motor to effectively power the motor. The driver chip itself can be used to power two low-voltage motors at once. The chip itself requires 2-7 V, whereas the motor must be powered using up to 11 V.[3]

The USB-6001 Malfunction I/O Device is a Data Acquisition (DAQ) and functions to process electrical and physical values, such as voltage, current, temperature, pressure, or sound in conjunction with a computer. This specific model is a low-cost device, which offers analog I/O, digital I/O, and offers basic functionality, such as data logging, portable measurements, for use cases of academic lab experiments. The DAQ is 14-bits and offers easy terminal connectivity, by using a screwdriver, to securely fasten wires which connect to the breadboard. [4]

Pulse Width Modulation (PWM) motor control is as the name suggests a motor control which works in unison with the motor in a series of ON-OFF switch pulses, that varies with a duty cycle, that controls the fraction of time that the output voltage is ON, as compared to when the voltage is OFF, while keeping the frequency constant. The power supplied to the motor can be varied by adjusting the width of the motor pulses. By changing this value, the speed of the motor can be controlled . The wider the pulse width, the greater the average voltage, and in turn the faster the motor will rotate. [5]

Through the various options of PWM control available, to control the motor, PD control was selected. Proportional Derivative (PD) Control, works to reduce overshoot and the settling time overall [6]. The closed-loop transfer function is modeled as the following:

$$T(s) = \frac{X(s)}{R(s)} = \frac{K_d s + K_p}{s^2 + (10 + K_d)s + \left(20 + K_p\right)} \qquad \text{Eqn. (1)}$$

The PD control serves to reduce overshoot and settling time and has a negligible effect on the rise time and steady-state error, this model is well suited to the implementation of the prototype as a whole.

2.0 MECHANICAL SYSTEM

2.1 Initial Concepts

The team developed a systems interfaces flowchart, to determine what the relative systems in the follower robot are, and how they will interact with the outside. Figure 1 shows the system flow chart.

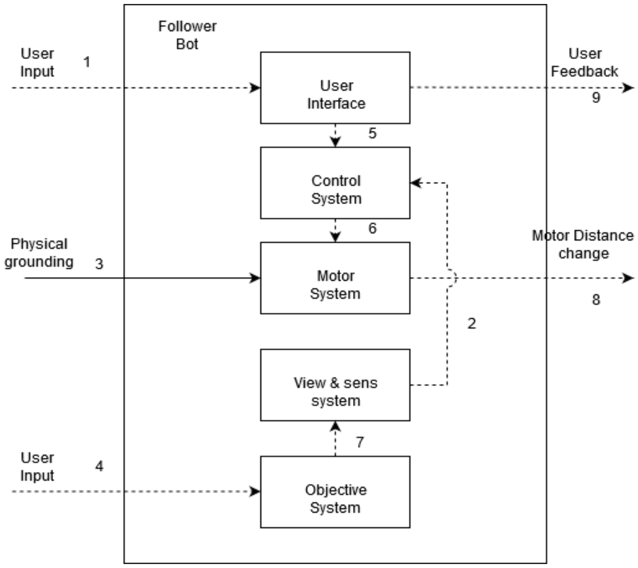

Figure 1: Presents the system interfaces.
Note that dotted lines represent data and solid lines are physical entities.

The system flowchart I/O:
1 & 4 - User Input: The user can either turn the device on/off, set the desired hold distance, or even visualize the control system I/O. The user will also be controlling Block B (in the objective system).
3 - Physical grounding: The device will need some sort of traction with the ground, if any motion is to take place.
9 - User Feedback: Will be LabView charts and distance data.
8 - Motor Distance Change: Is the response of the system to changes in its surroundings, regarding the objective system.
2 - The sensor inputs must be conditioned, and used as part of the motor control system, before power can be sent to the motor.
5 - The user interface is how the user can place the control system parameters.
6 - The control system will include some sort of PID variant, and will be used as the motor control system. This will translate sensor inputs, to motor outputs.
7 - The objective system can only interact with the rest of the system through the sensor system.

After determining the relative systems, a morphologic chart was made from embodiments of the different subsystems in Table 1. Below a clean rendering of the morphologic chart developed is shown in Table 1. Information is then extracted from Table 1 to determine the best combination of subsystem designs to be used. Since the LabView user interfaces were still unfamiliar to us at the start of the design, the user interface subsystem was not included in Table 1.

Table 1: The morphological chart of various subsystem designs.

SubSystem	**Design 1**	**Design 2**	**Design 3**	**Design 4**	**Design 5**
Control	PID	PD	P	LEAD/LAG	-
Motor	Wheel on rail	Wheel on Ground	Continuous Track (Think Tank Wheels)	Rack & Pinion	Ball Screw
View & Sensor	On Follower	On Objective	On Ground	-	-
Objective	Paper Slide on Rail	Block On Rail	Free Block	-	-

Note:All dashes mean that there was no more designs given.

Control : Due to project requirement and complexity, lead/lag compensation was omitted. The design was left open till the end on what kind of PID. Finally A PD was used, since the robot had no consistent error that would need an integrator to correct for.

Motor : The car design (wheel on ground), even though easy, was taken off immediately from suggestions during class time. Ball and screw showed cost problems. Rack and pinion was the next best viable solution after a ball screw. The design has little slack, and very accurate control.

View and sensor: On follower was chosen to simplify relative calculations when using LabView. This proved to be a good choice, as not having the sensor move will mean that the control systems set values needs to be continuously changed.

Objective : Paper slide on rail was chosen as building it with acrylic sheets was easiest. The concept design, even though was rushed to achieve the deadline, we needed to make sure a design would be chosen where its behaviour would be predictable and sufficiently versatile. The reasoning being that we needed to make sure we would not run into any major setbacks, and even if any came up the design would allow for quick and major adjustments.

2.2 MECHANICAL DESIGN

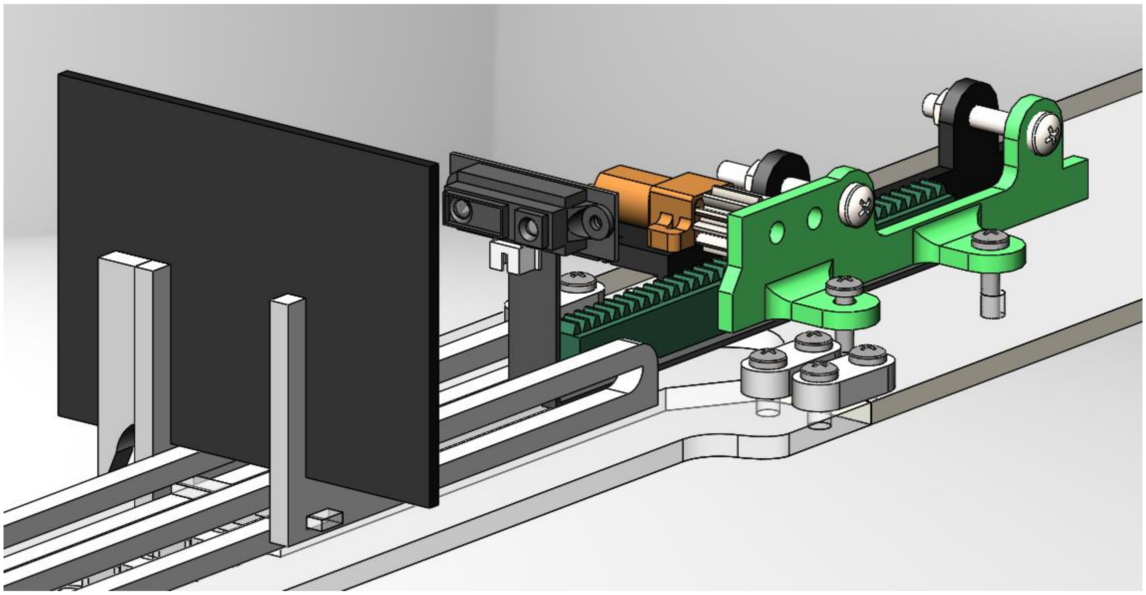

Figure 2: Solidworks CAD Model of Rack & Pinion Design

The rack is attached to the Sharp IR Sensor and is actuated by the pinion connected to the shaft of the motor. This design was implemented due to its effortless controllability and precision. The light weight of the rack along with the small pinion gear reduces the torque required by the motor to move the system. Since the rack and pinion are meshed indefinitely during the operation of the system, slack is compensated by the motor and is a benefit of the design. The 1:1 gear ratio is effortless to troubleshoot and minimizes the frictional losses that would have been added by the addition of other gears. Since the acrylic has a small coefficient of kinetic friction ($\mu = 0.15$) [8], it was also designed and laser cut to form a rail system for the movement of the black paper acting as Block B.

The rack is made of hard plastic and the pinion is made of casting steel which is durable and resistant to chipping. A 5mm acrylic was laser cut and folded to support the rack and hold the IR Sensor about 4 cm off the base of the assembly. 5mm acrylic was also laser cut to form the base plates that hold the entire structure together. M4 and M5 Type 1 cross recessed screws along with M8-32 keps nuts were used to connect the different components of the system together. Detailed CAD of each individual part can be found in Appendix 2**.** In summary, the entire system is approximately (52x60x10)cm.

The rack and pinion design was chosen because of its simplicity and controllability. The torque required by the motor was calculated (Appendix 1**)** to be approximately 76.1 μNm to move the rack along its track. The motor's stall torque is 266 µNm as specified by the manufacturer; therefore, the operating torque is far less than the capacity of the motor.

It was noticed that the initial 3D printed side plate sheared due to the 3D printer setting.The printer printed in the direction orthogonal to the force that was applied to the first hole due to the shaft of the pinion. As a result, the material sheared along the yellow line. Super glue was used to reattach the broken piece, however, the group decided to print another model with filleted corners to spread out the stress and a 45 degrees print offset to prevent shearing.

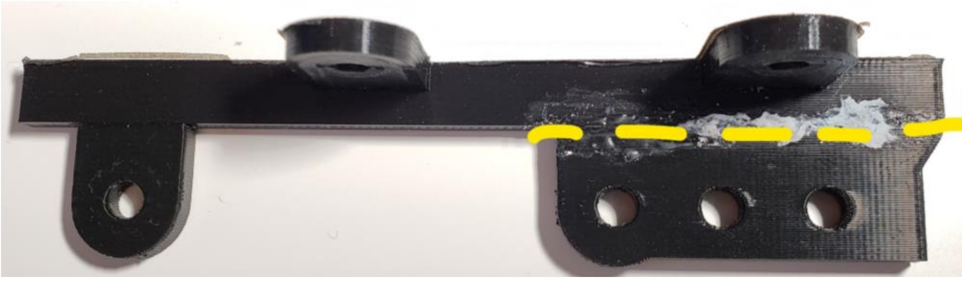

Figure 3: Sheared 3D printed side plate

Another noticeable problem was the slack that was created by the shaft hole on the pinion. The motor shaft is a cylinder with a key slot, however, the pinion slot is square, therefore, paper clips were used as shaft keys to attach the pinion to the motor shaft.

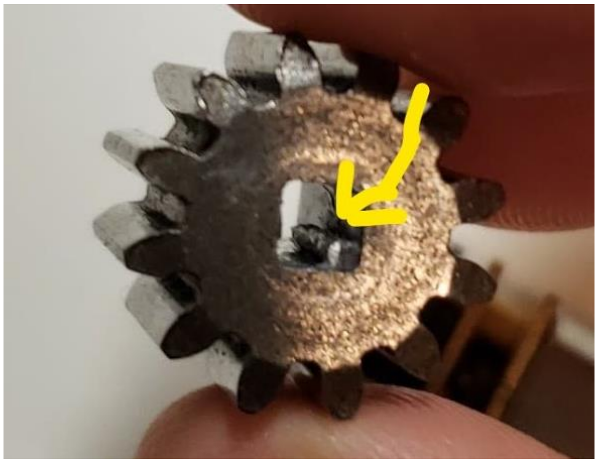

Figure 4: Paper clips were stuck on the corners of the pinion to act as shaft keys

Altogether, the design was durable throughout the calibration process because the CAD model allowed us to identify any problems pre manufacturing. The rack and pinion proved to be a good mechanical design to complete this project.

3.0 ELECTRICAL SYSTEM AND DATA ACQUISITION

3.1 Model of Wiring

The wiring setup was mainly guided by the motor driver inputs. The Control table for the driver, can be seen below. Based on this and various pin locations on the USB - 6001 DAQ we have made the wiring in Figure 5. Shorter wires, and noise reduction were used. The whole system is grounded to the mains power.

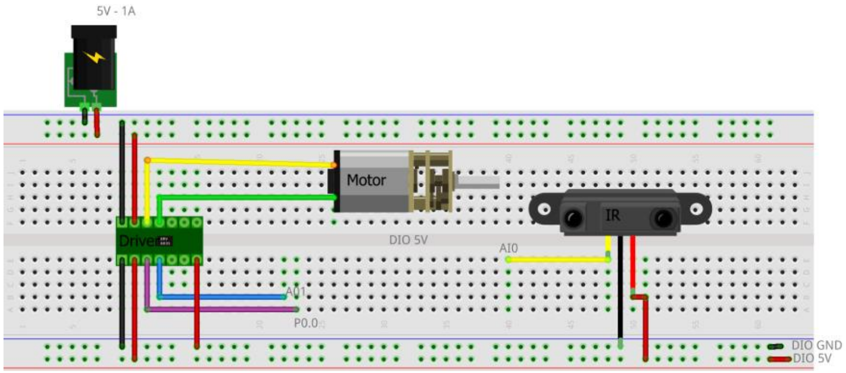

Figure 5: Breadboard view of the wiring. Note that all power wires were twisted together, and all text markings present a port of the USB - 6001 DAQ.

There are a few key wiring notes that should be kept in mind. First is that the PWM signal going to the Drivers Enable pin needs to be an analog output. The opposite is true for the phase pin, it needs a digital input. The setting for the PWM itself is presented under LabView program description. The motor connection is arbitrary, but it will work opposite to what was intended if wired wrong, the solution is to just switch the pins. Finally note that the DAQ cannot on its own supply enough power to run the motor at its peak performance. Finally the motor and sensor / DAQ grounds are isolated from one another. There for the sensor / DAQ side is grounded with the PC ground, and the motor is grounded to mains power directly. This may not be the best idea, since the system is fully floating on one side, especially if connected with a laptop.

3.2 Sensor calibration

The IR sensor was calibrated statically and the system as a whole was calibrated dynamically. The results of the calibration are shown in the Results and Evaluation. Here we explain the actual process.

I. Static Calibration

The static calibration was done by performing 5 cycles of the sensor through the full range of block B’s movement. The cycles were then used to find the sensitivity, nonlinearity error, repeatability error and hysteresis error.

The measurement from the sensor was not linear, and therefore some values like sensitivity have been presented as equations instead of numbers.

II. Dynamic calibration

The dynamic calibration process, was done by quickly moving the B block, and viewing the response curve of the sensor. Note that this calibration is done without the motor being active. An overall measurement of response time was also given. This measurement was done on a stopwatch due to complexities in bringing the measurements in code.

3.3 Signals

Table 2. Shows the signals needed to drive the motor driver.
The Main Signal that needs particular attention is the operation of the DC motor driver. Table 2 shows the motor drivers operation that was implemented. The IR sensor itself only needs a VCC power and ground and a V_{out} to the DAQ for reading the distance signal.

Table 2: Signal chart to drive the motor

Drive / Break Operation for Motor Driver			
X - Phase	X - Enable	OUT 1	OUT 2
0	PWM	PWM	L
1	PWM	L	PWM
X	0	L	L

4.0 CONTROL SYSTEM

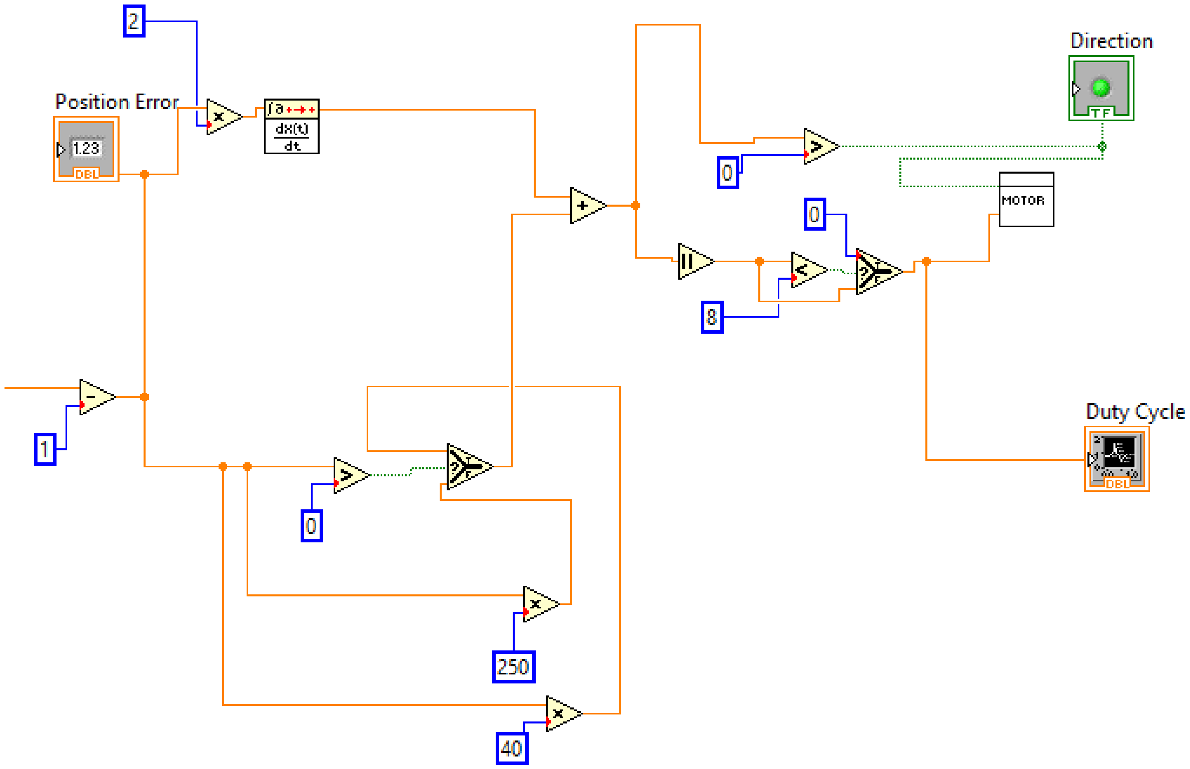

Figure 6: Block Diagram of the Control System implementing PD Control

The control system implemented in the LabVIEW program allows for variable speed control in the operation of the robot allowing for smoother operation. This is done using PD control. The input variable into the control system is the position error of the follower block in cm determined in the sensor subVI. The P control is first implemented using two different gain values determined through experimentation. These were found, ideally to be 40 for a positive position error (follower block is too far away) and 250 for a negative position error (follower block is too close). The signal is multiplied by both gains separately and a selector block is used to decide which signal is implemented (40 gain if it was positive and 250 gain if it was negative). At the same time another branch of the program is used to implement D control. This branch simply applies a gain of 2 to the signal then finds the derivative of the error using a derivative block. These two signals are added to each other to obtain the final PD controlled position error. Finally, the sign of the position error is output to the motor subVI to determine its direction and the absolute value of the position error is output to the motor subVI to determine its duty cycle.

In order to reduce fluctuations in the follower block at steady state, a deadband was implemented. This simply outputs a value of 0 to the duty cycle of the motor if the position error is very small (8 after PD control, determined experimentally)

The equations for the PD control implemented in the control system for positive and negative signals can be represented through equation 2 and 3 as:

$$u(t) = 40e(t) + 2\frac{de(t)}{dt} \qquad \text{(Eqn 2)}$$

$$u(t) = 250e(t) + 2\frac{de(t)}{dt} \qquad \text{(Eqn 3)}$$

Where e(t) is the input position error and u(t) is the PD controlled position error.

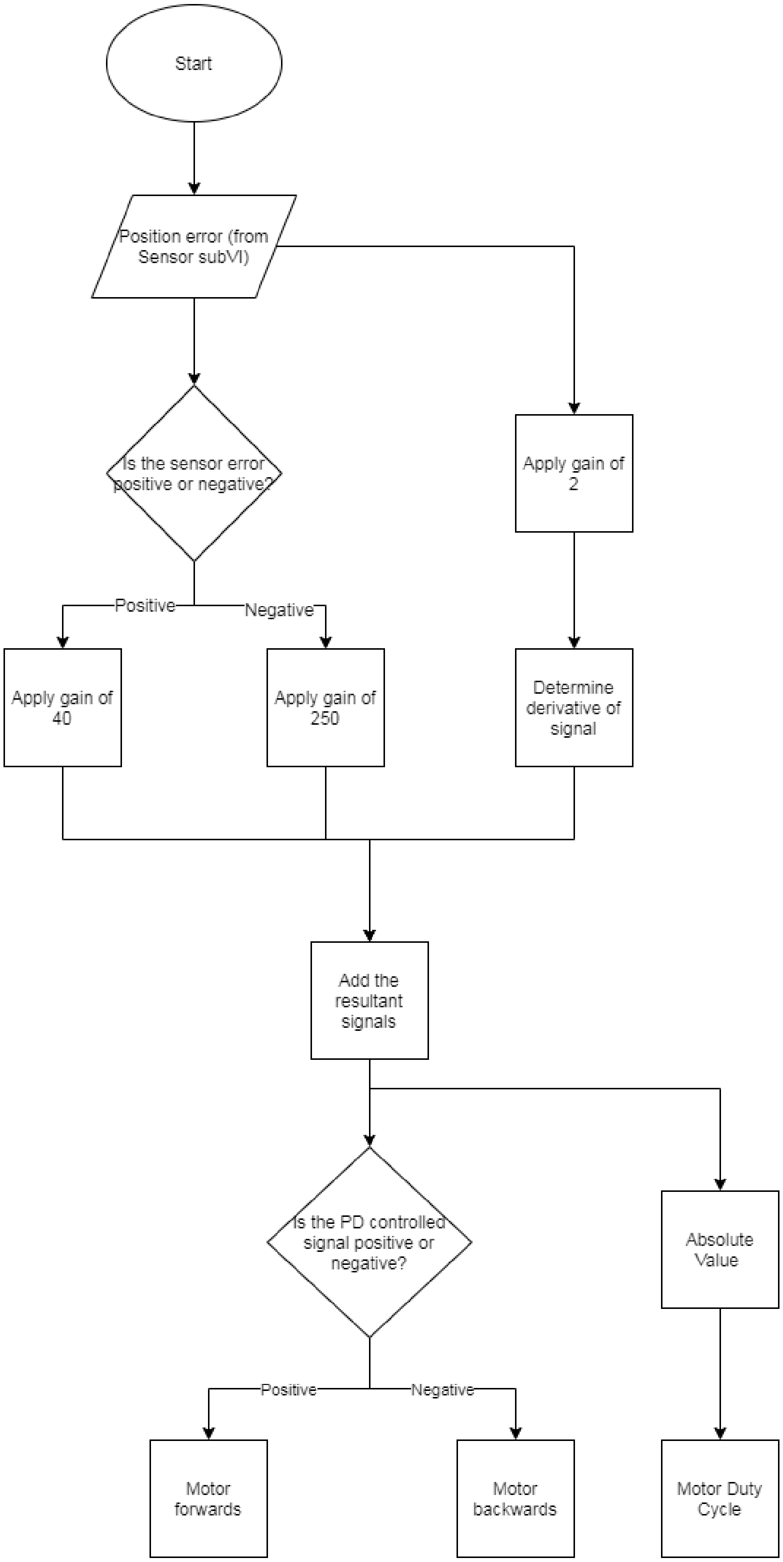
Start
Position error (from Sensor subVI)
Is the sensor error positive or negative?
Apply gain of 2
Positive
Negative
Apply gain of 40
Apply gain of 250
Determine derivative of signal
Add the resultant signals
Is the PD controlled signal positive or negative?
Absolute Value
Positive
Negative
Motor forwards
Motor backwards
Motor Duty Cycle

Figure 7: Flowchart of PD Control System

4.1 Labview Program Description

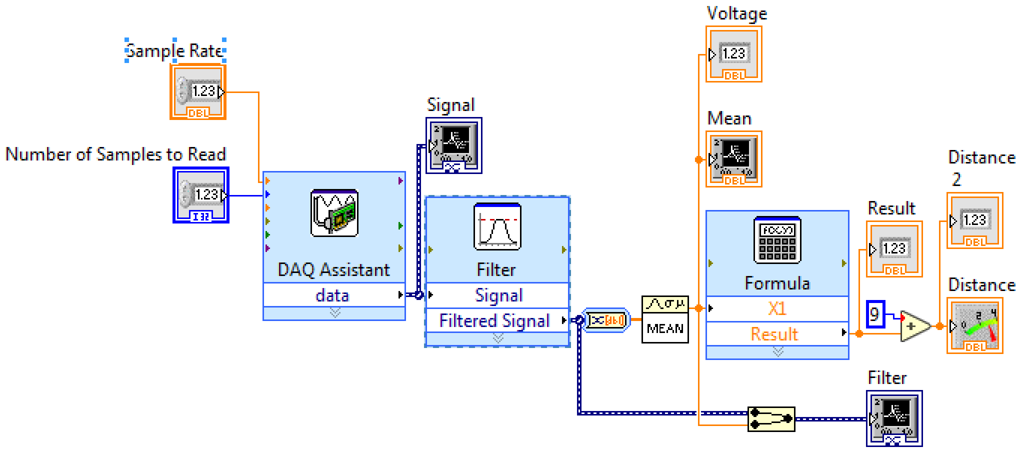

Figure 8: Sensor SubVI

4.2 Sensor Sub VI

The Sensor sub VI, is responsible for reading in the sensor output, filter the signal and also run it through the sensitivity calibration. The output of the sensor is a distance from block B, shown on a dial. The filtering process will be explored deeper in the results and evaluation section. For now each VI is explained individually. The various graphing VI's will not be explained as they are self explanatory.

DAQ Assistant : Will Read data from the USB 6001 analog input pin.

Filter : Will condition the signal with a 12 point smoothing filter.

Formula : Includes the sensitivity formula from the static calibration results, subtracted by an offset to give real world distances.

Note that the data is averaged several times for easy representation visually.

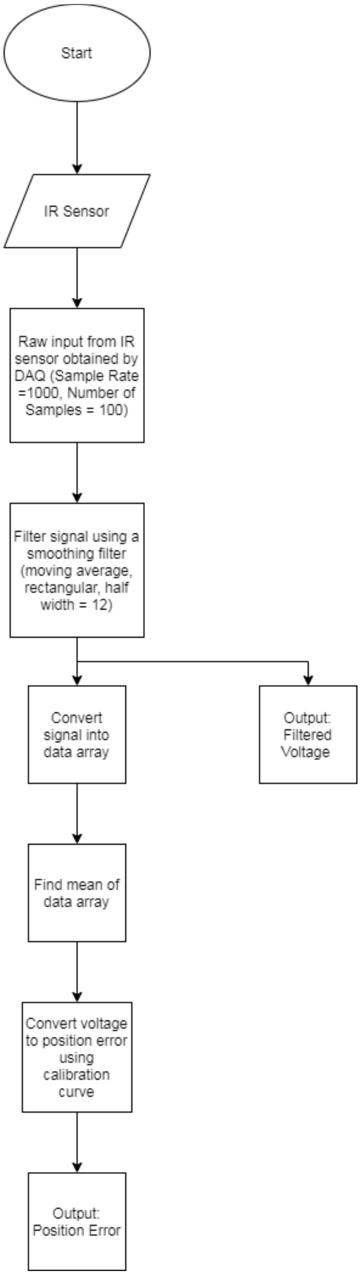
Start
IR Sensor
Raw input from IR sensor obtained by DAQ (Sample Rate =1000, Number of Samples = 100)
Filter signal using a smoothing filter (moving average, rectangular, half width = 12)
Convert signal into data array
Output: Filtered Voltage
Find mean of data array
Convert voltage to position error using calibration curve
Output: Position Error

Figure 9: Flowchart of Sensor SubVI Operation

The Sensor sub Vi is presented as a flowchart in Figure 8. Here the start and out sections will be connected to other VI's . The presentation shown here as with the others, is if the VI was used on its own. Further note that the Flow chart shows several data type conversions. These are done automatically by LabView and may not be reproducible on older versions. However as long as you make the data types match, no problems should arise.

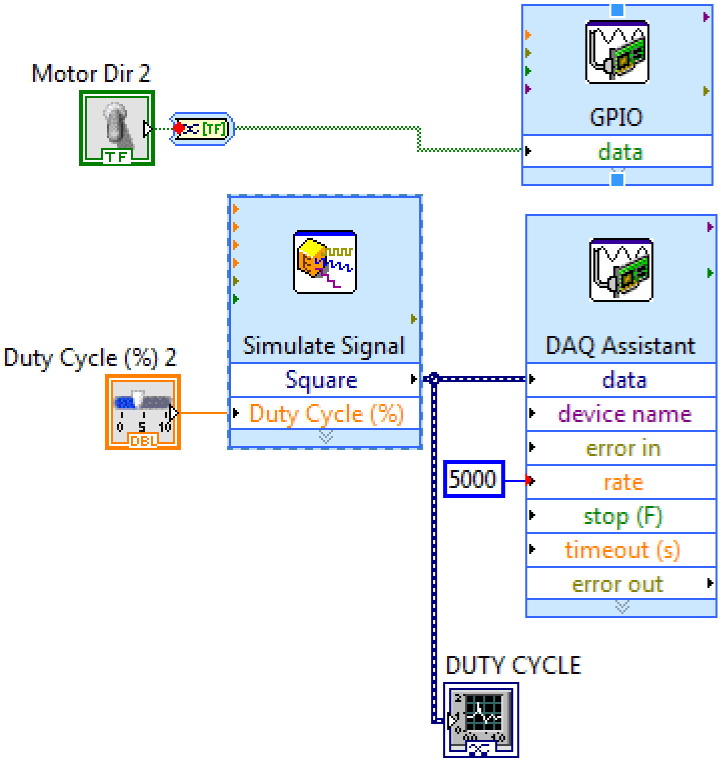

Figure 10: Motor SubVI

4.3 Motor Sub VI

The motor sub VI, is only used to control the motor driver, and not the motor itself directly. The VI uses to DAQ assistants, one named GPIO and the other DAQ Assistant. The need for two is that the first will give a digital on/off signal, while the latter sends an analog output. Many Different motor options, such as speed and direction or even the frequency of the duty cycle are controlled here (50Hz).

Simulate Signal : Outputs a PWM 0-5 V signal at 50Hz with a sample rate of 500 samples/sec. The Unit has been made to allow easy control of Duty Cycle by a controller.

GPIO : Can be given a T/F input to change motor direction. The unit send a digital high or low output.

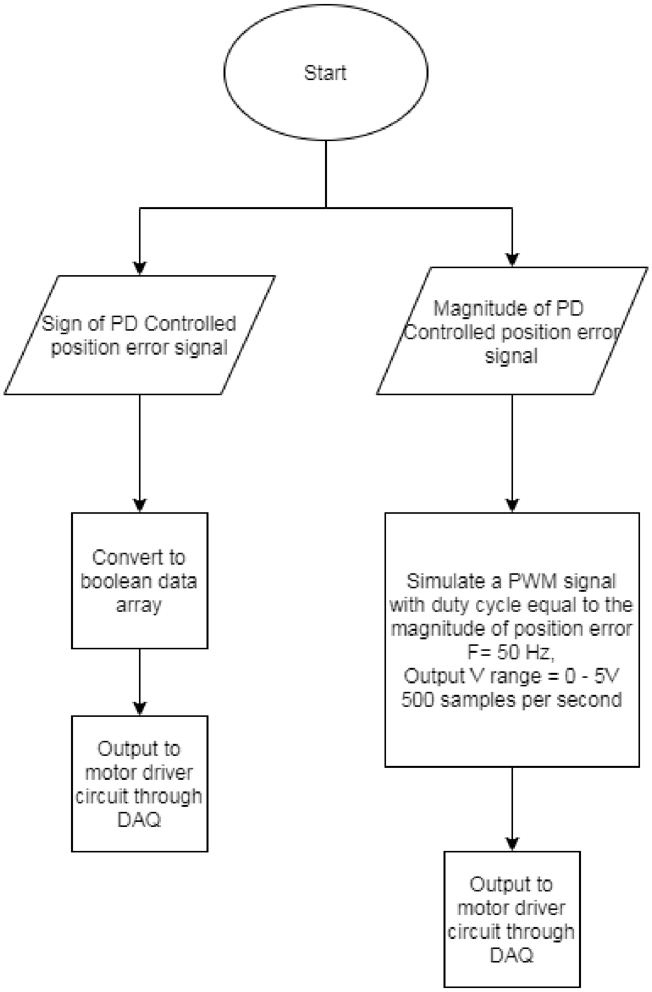
Start
Sign of PD Controlled position error signal
Magnitude of PD Controlled position error signal
Convert to boolean data array
Simulate a PWM signal with duty cycle equal to the magnitude of position error
F= 50 Hz,
Output V range = 0 - 5V
500 samples per second
Output to motor driver circuit through DAQ
Output to motor driver circuit through DAQ

Figure 11: Flowchart for Motor SubVI Operation

As can be seen in Figure 10, the Motor SubVI is directly connected to the PD controller. The Controller can give Motor VI commands in two ways, either direction or duty cycle. The VI, used a + / - conversion to T/F for direction and the PD controller itself for Duty cycle.

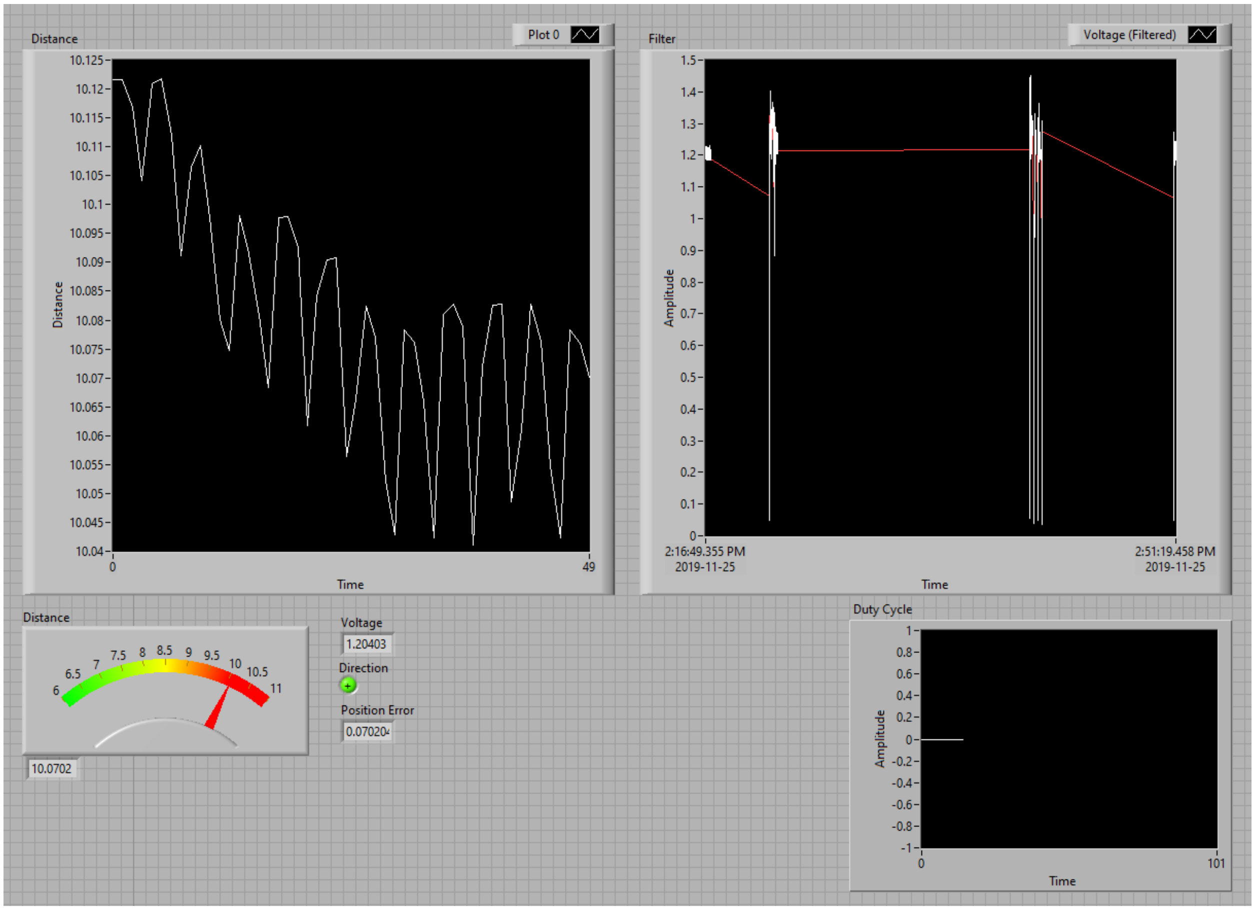

Distance 10.0702

Voltage 1.20403

Position Error 0.07020

Figure 12: Front Panel of Main Program

The front panel of the program uses graphs and indicators to display necessary information to the user. In particular, the front panel uses a distance dial to give a visual representation of the distance between the blocks as well as displaying the numerical distance value underneath. The program also has indicators for the sensors output voltage and position error. A light indicator is used to display the motor direction, with the light being on representing forward rotation and off representing backward rotation. Finally there are two waveform graphs which display the output voltage of the sensor and the duty cycle of the motor to allow the user to see how the motor's variable speed responds to different magnitudes of distance variation for the sensor.

5.0 Results & Evaluation

5.1 Static Calibration

I. Calibration results

Table 3: Shows the static calibration results in Voltage and percent FSO (5V)

Error	±Voltage	%FSO
Non Linearity	0.0045	0.3%
Repeatability	0.005	0.33%
Hysteresis	0.01	0.66%
Sensitivity	OFFSET - $(-18.974 * V^2 + 49.836 * V - 20.827)$	
Overall	**±0.0121 V**	**0.80%FSO**

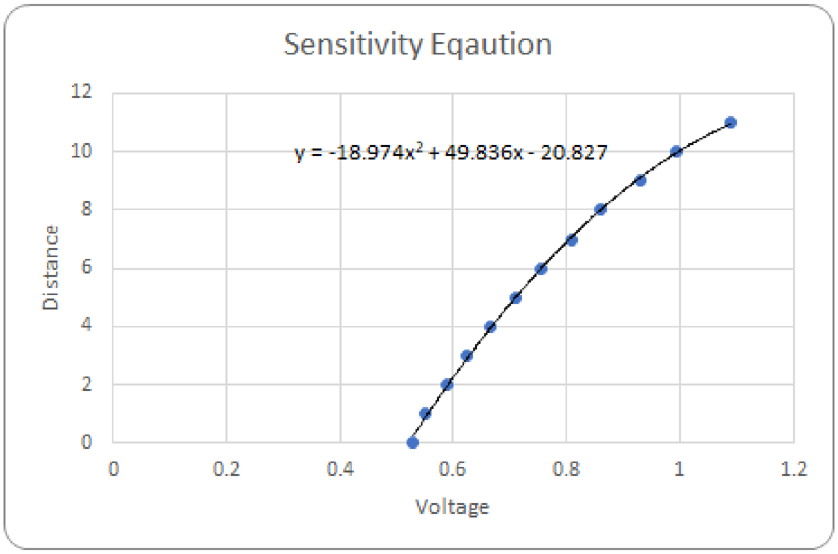

Figure 13: Shows the sensitivity Fit to a 2nd order polynomial.

Note because of the non-linear nature of the sensor and the gap of 9 cm before readings are calibrated, zero offset error is not reported. Same goes for sensitivity, it is reported as an equation of a line of best fit. The overall uncertainty of the sensor is as follows:

$$\sqrt{0.0045^2 + 0.005^2 + 0.01^2} = \pm 0.0121\, V$$

The overall error of the sensor is presented as **±0.0121 V or 0.80%FSO.**

II. Process of calibration

The calibration was performed on a cycle of data values taken at 1 cm intervals. The values were taken at the full operating range of the sensor, meaning we excluded the 0 - 9 cm distance. Considering the large operating gap, the actual block A - B distance (fully retracted) was placed to be at about 9 cm. This would allow the largest operating range. As noted above the sensitivity calculation was done with a 2nd degree polynomial fit in excel, with no forced zero. The data for the fit was taken from the average of all cycles put together. Note that the sensor has a bias because of the sensor properties of 9cm however this isn't reported as a zero offset error (as the start isn’t actually 0cm). Nonlinearity was taken as the max deviation of each measured value to the expected value taken from the sensitivity equation. Non-linearity here is a measure of deviation from the 2nd degree poly fit and not a line. Hysteresis was taken as deviation between up - down measurements from down - up. The greatest deviation was taken as Hysteresis error. Repeatability was also taken as greatest deviation from average of each centimeter value, to each measured centimeter value.

5.2 Noise and other sources of error

Even though a 12 point moving average filter has a distinctive frequency response that may undesirable, running the sensor output through a FFT did not show a frequency chart. Due to this issue and also failures in randomly assigning cutoff frequencies, the moving average filter was used. Not that the results still were good enough to allow for a fully functioning follower.

Without identifying all sources of error, we used simple moving averages, and adjusting calibration measures to real world measurements in order to fix any noise and error issues. Overall this means that our method was one of trial and error, but it did give the needed results.

One of the most important sources of error, was the IR sensors calibration curve, even though the results were highly reproducible after the polynomial fit, the sensors close range errors would completely throw off the PD controller. For this a physical block was included in front of the sensor, to stop the B block from coming to close. This issue is a common problem with most distance sensors, however the error in our particular one was much higher than stated. About 9 cm and below would produce erroneous results. This wasn’t a problem too much, because the design was meant to hold a distance of 10cm.

Table 4: Dynamic Calibration Results

Settling Time	8 ms
Rise Time	17 ms
Steady State	10.01 cm

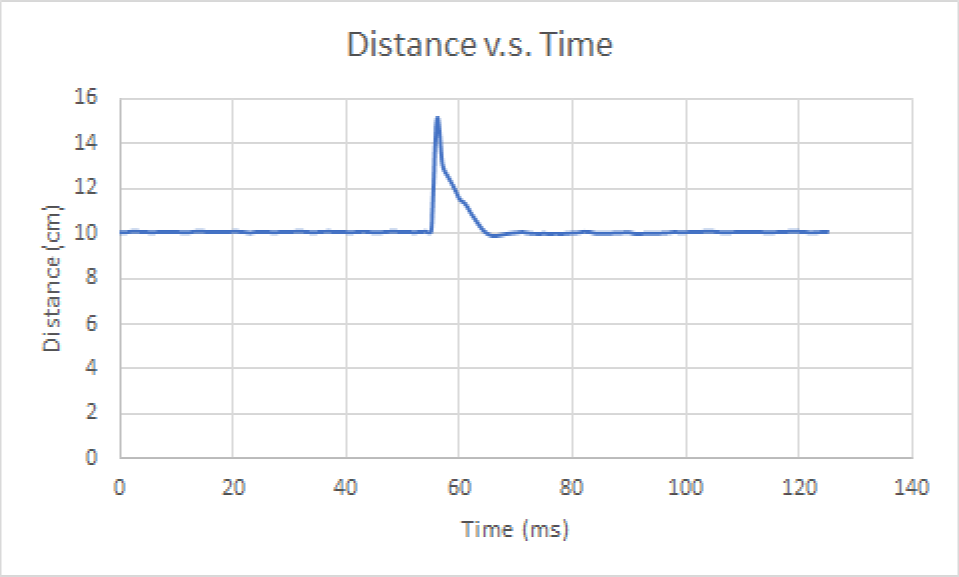

Figure 14: Step Response of the System (Distance)

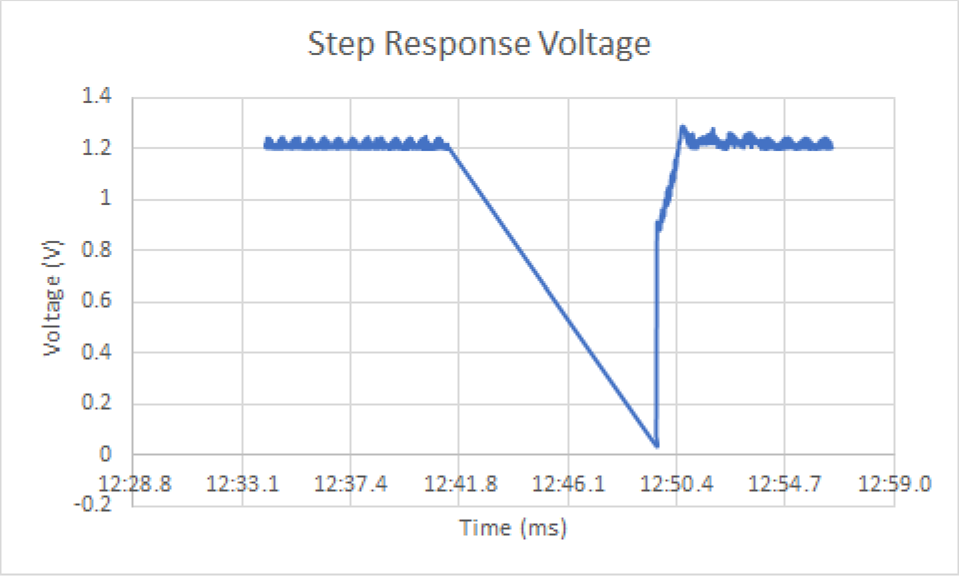

Figure 15: Step Response of the System (Voltage)

Dynamic calibration was performed by placing the block a fixed distance away from the sensor (5 cm) and running the program allowing the follower to respond instantaneously to the 5 cm separation simulating a step response. Through this it was determined that the rise time of the system response is approximately 17 ms, as the system was able to reach 90% of its steady state response within this period of time. The settling time was reported as 8 ms, as the system was able to settle within 99% of its steady state value within this time period.

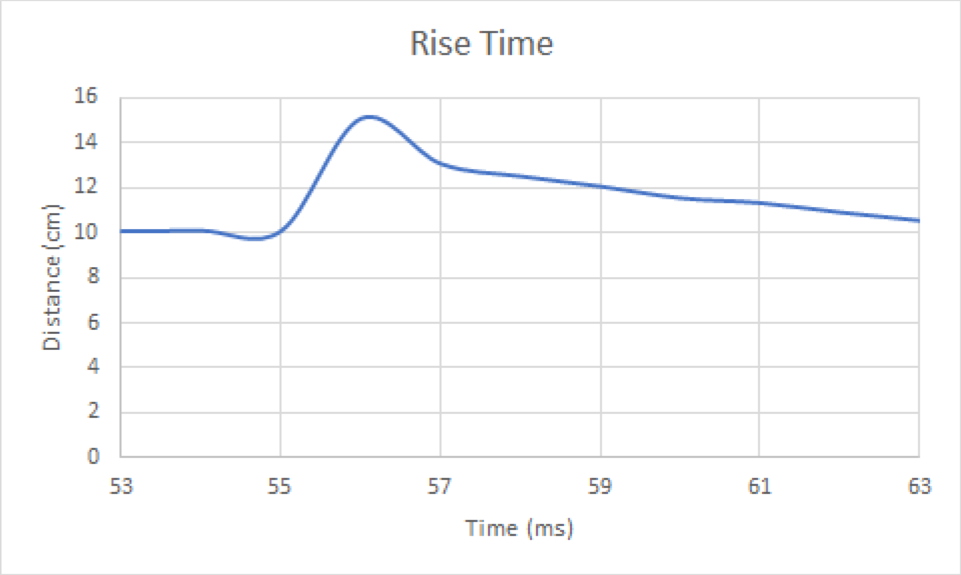

Figure 16: Rise Time of the system response with a step input of 5 cm

This graph shows the system response to the step input, observing the data it can be seen that the response reaches 90% of its steady state value within 8 ms.

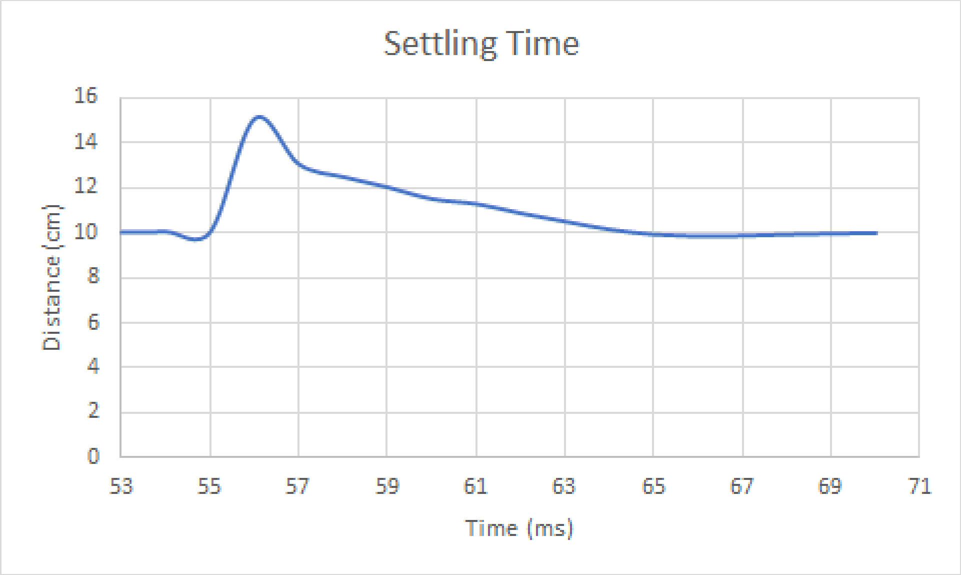

Figure 17: Settling Time of the system response with a step input of 5 cm

Observing the steady state portion of the step response it can be seen that the response settles within 99% of itself within 17 ms.

6.0 Discussion

The rack and pinion proved to be a good design choice to complete this project. By using acrylic and 3D printing the mechanical structure, it was noted that the design only showed unexpected results in terms of response time. The unit would respond to a stimulus with a one second delay. The first assumption was that the system may be under large friction and the input duty cycle isn’t strong enough. This does not hold well since the systems duty cycle usually starts at 100%. A likely problem is the DAQ itself, it is writing data to the Motor at 5000Hz, while reading the IR sensor data at 1000Hz. Even though we could not change these settings without getting errors and test the hypothesis; by looking at the USB-6001 manual [7], we concluded that the system can read at 20kS/s and write at 5kS/s. Notably the read speed is no where close to the maximum but the write speed is exactly at our designated 5000Hz. This can definitely cause a problem in response time of the system. It should be noted that the set value of 5000Hz was not chosen arbitrarily, the higher write rate would allow for a well rendered square wave being given to the motor. This would cause the motor to run much faster.

Another problem that came into effect after we damaged the original motor supplied. It seems several rounds of soldering had weakened the magnets inside the motor, as after getting a new motor the system started to oscillate and not stabilize. To solve this issue a band stop was added to the LabView program. This managed to hold the motor stable.

7.0 Conclusion

The process of developing the linear tracker, many different aspects regarding mechanical design, electrical design and programming were considered. The benefits and hindrances of using a rack and pinion design were apparent. The rack and pinion design is very effective in following the block as the motor rotation can easily be translated into displacement through well meshing gears. The rack and pinion is also successful in achieving linear motion and has only minor friction with the rail system of the design. There are also some limitations however mainly being the length of the rack. The rack and pinion runs off the rails if the follower is brought too far out and runs out of rack if brought too far back. This design flaw could be improved through increasing the rack length. The sensor used for the linear tracker was found to give accurate readings which were successfully converted into position error readings and allowed for the system to respond accurately to distance changes. The sensor also limits the operation however through its calibration curve. The calibration curve of the sensor prevents readings too close to the sensor, this causes issues when bringing the block back towards the sensor as bringing it too close causes error in the conversion to position error and subsequently causes the motor to react incorrectly. A solution was implemented in the form of a physical block which prevented the block from being moved backwards too close to the sensor. A better solution would be to modify the sensor calibration and PD control implementation until the physical block is as small as possible allowing the full range of the sensor to be used. The electrical design of the linear tracker was also implemented with success. The wiring of the design was organized and did not interfere with any mechanical components of the system. A design improvement which could improve the accuracy of the system is driving the motor directly rather than requiring an intermediate motor driver circuit. Since the DAQ is not able to produce enough power to the motor it was necessary to use an external power source. Additionally the program has issues synchronizing with the motor actuation at times and results in the motor continuing to run after the program has been stopped. Using a less powerful motor or using a different DAQ which could supply power to the motor would reduce noise and make the motor operation more accurate. The programming of the linear tracker was found to be effective in achieving its objective and was organized into 3 clear subsystems (Sensor, PD Control, and Motor). The program requires a sensor reading to be filtered, converted to a data array, averaged, converted to position error through a calibration curve and PD controlled in order to finally achieve motor actuation. Each step of the process introduces minor delay so reducing the steps or finding premade blocks which achieve these functions more efficiently would be effective in improving the program design. The program response could also be improved by implementing PID control instead of only PD as the addition of integration would improve speed control even more and allow for faster operation. Altogether, this project proved to be a good learning opportunity.

8.0 References

[1] Design Project Outline – MEC 751 Design Project F19. (n.d.). Retrieved November 24, 2019, from https://courses.ryerson.ca/d2l/le/content/309396/viewContent/2632700/View

[2] Pololu - 298:1 Micro Metal Gearmotor HP 6V with Extended Motor Shaft. (n.d.). Retrieved from https://www.pololu.com/product/2218.

[3] Pololu - DRV8835 Dual Motor Driver Carrier. (n.d.). Retrieved from https://www.pololu.com/product/2135.

[4] USB-6001. (n.d.). Retrieved from http://www.ni.com/en-ca/support/model.usb-6001.html.

[5] Pulse Width Modulation Used for Motor Control. (2018, February 16). Retrieved from https://www.electronics-tutorials.ws/blog/pulse-width-modulation.html.

[6] Introduction: PID Controller Design (n.d.). Retrieved from http://ctms.engin.umich.edu/CTMS/index.php?example=Introduction§ion

[7]National Instruments (n.d.) USB-6001 Retrieved November 20, 2019 from https://www.ni.com/en-ca/support/model.usb-6001.html

[8] MSC.Adams. (2008, August 8). Material Contact Properties Table. Retrieved November 25, 2019, from http://atc.sjf.stuba.sk/files/mechanika_vms_ADAMS/Contact_Table.pdf.

9.0 Appendix

9.1 Appendix 1: Torque calculation of motor

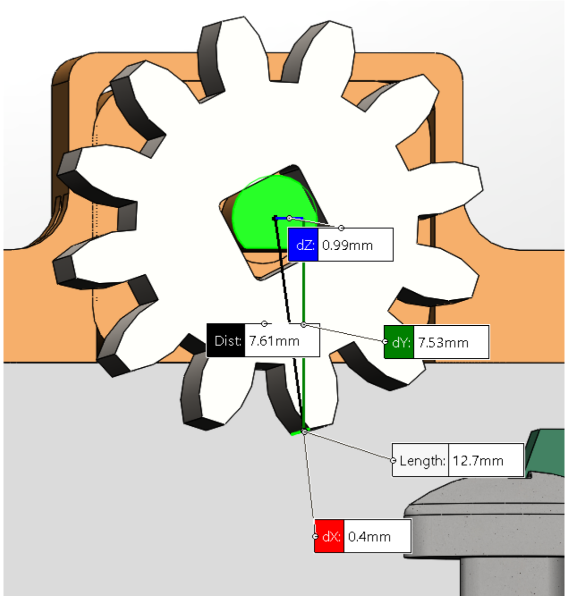

Figure 18: Pinion connected to motor

Assuming the rack travels the 10cm required distance in 1.5 seconds and weighs approximately 150grams.

$$T_{motor} = r_{pinion} * F_{rack}$$

$$T_{motor} = (0.00761m) * (0.150kg * \frac{1m}{15s})$$

$$T_{motor} = 76.1\ \mu Nm$$

9.2 Appendix 2: Materials and CAD Drawings

Table 5: List of materials
Note: CAD drawings not provided for standard parts

Part #	Part Name	Material	Quantity
1	Base plate	Acrylic 5mm	1
2	Side plate	PLA Filament hard plastic	1
3	Rack Bottom plate	Acrylic 1.5mm	1
4	Rack	Hard plastic	2
5	Pinion	Cast Steel	1
6	Train side plate	Acrylic 5mm	2
7	Train slider	Acrylic 5mm	2
8	Train base	Acrylic 5mm	1
9	Main plate	PLA Filament hard plastic	1
10	M4x0.7x20 Type 1 Screws	Metal	6
11	M4x0.7x5 Type 1 Screws	Metal	6
12	Standard Keps Nuts	Hard Aluminum	12
13	Straight Slots 5x7.5	Acrylic 5mm	3
14	Sharp IR Sensor	Plastic	1
15	298:1 6V Micro motor	Metal	1
16	Motor casing	Plastic	1
17	Motor mount screws (M1x4)	Metal	2

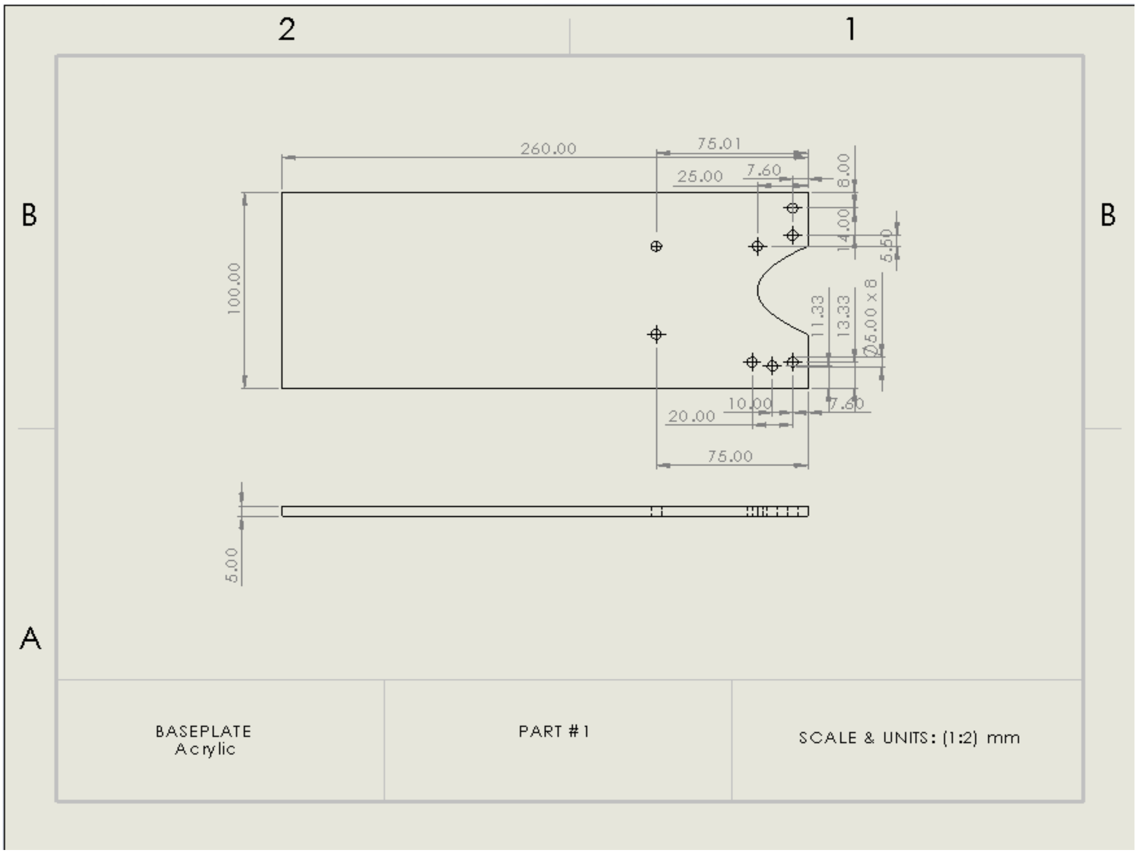
2
1
B
B
A
260.00
75.01
25.00
7.60
8.00
14.00
5.50
100.00
11.33
13.33
Ø5.00 x 8
10.00
20.00
7.60
75.00
5.00
BASEPLATE
Acrylic
PART #1
SCALE & UNITS: (1:2) mm

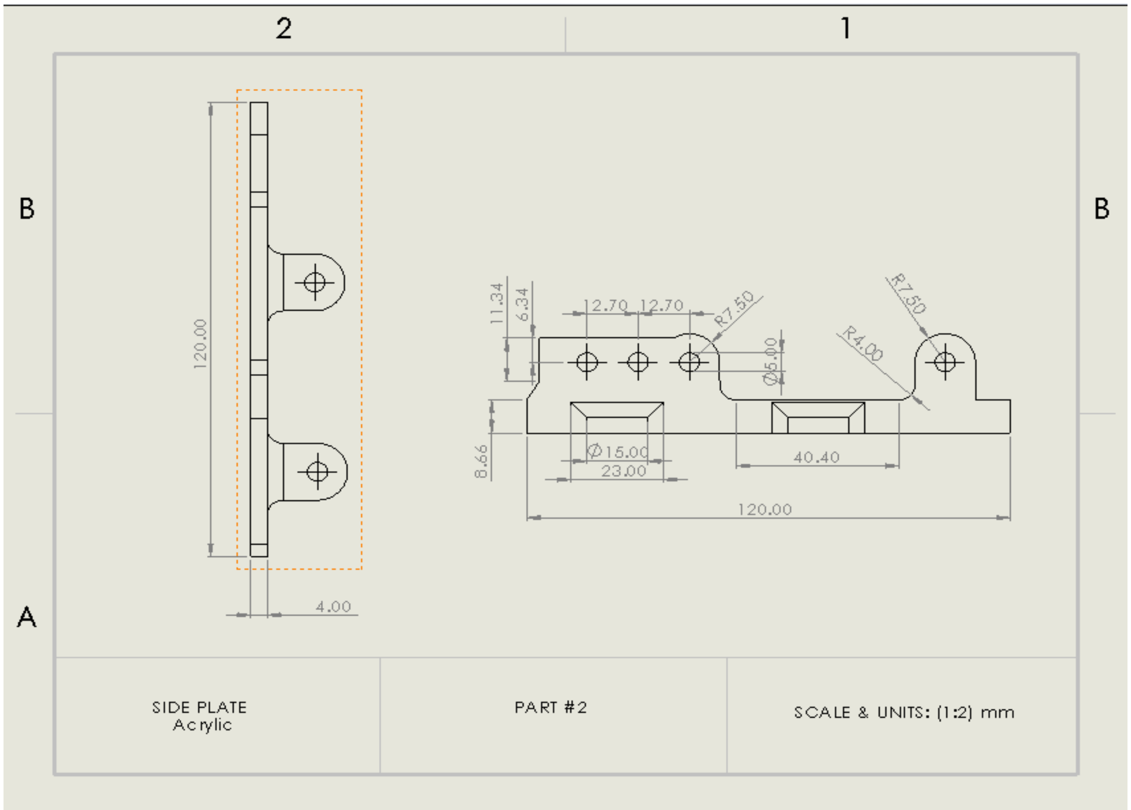
2
1
B
B
A
120.00
4.00
11.34
6.34
12.70
12.70
R7.50
R7.50
R4.00
Ø5.00
8.66
Ø15.00
23.00
40.40
120.00
SIDE PLATE
Acrylic
PART #2
SCALE & UNITS: (1:2) mm

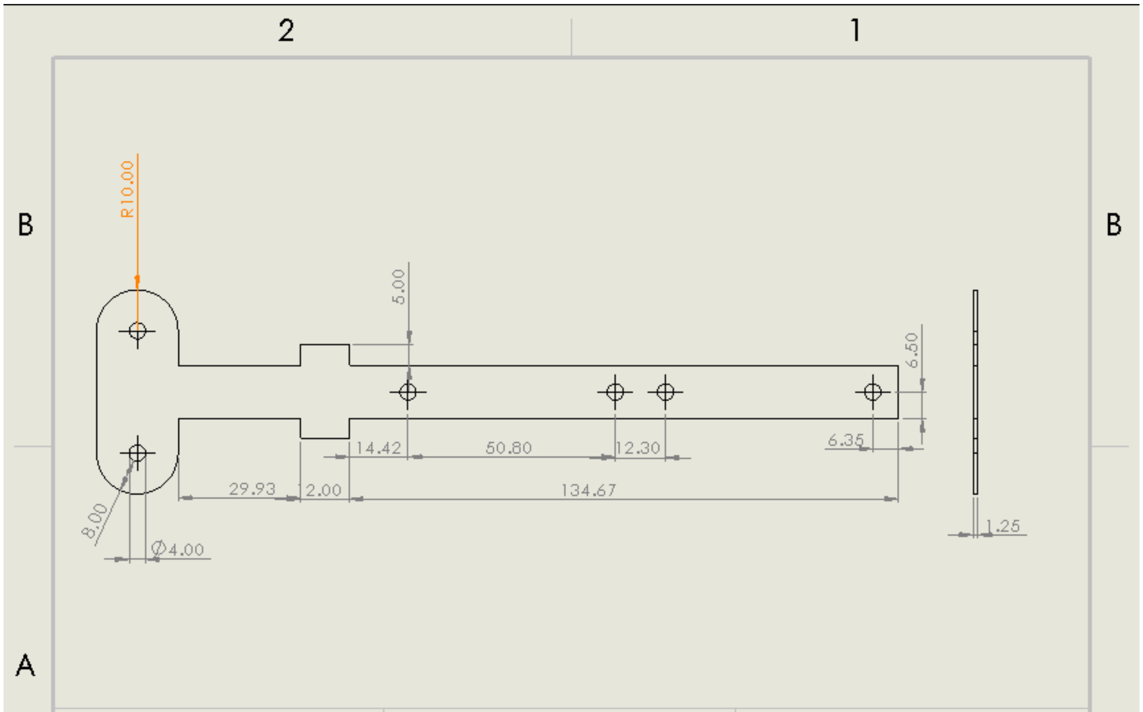

Rack Bottom Acrylic (1.25mm)	PART # 3	SCALE & UNITS: (1:1) mm

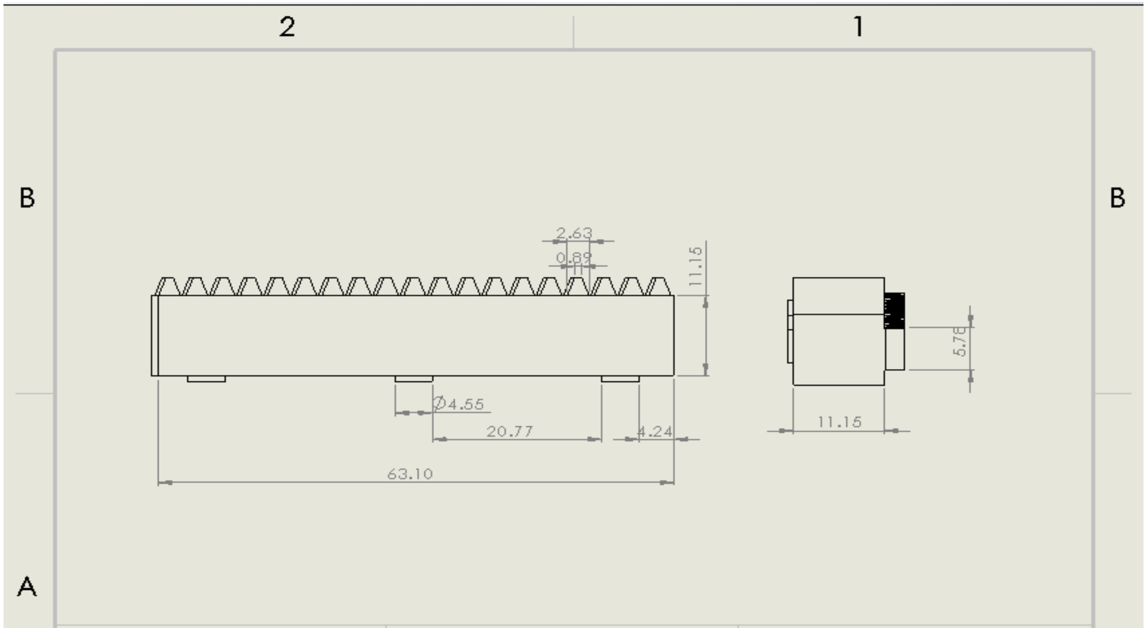

Rack Hard Plastic	PART # 4	SCALE & UNITS: (2:1) mm

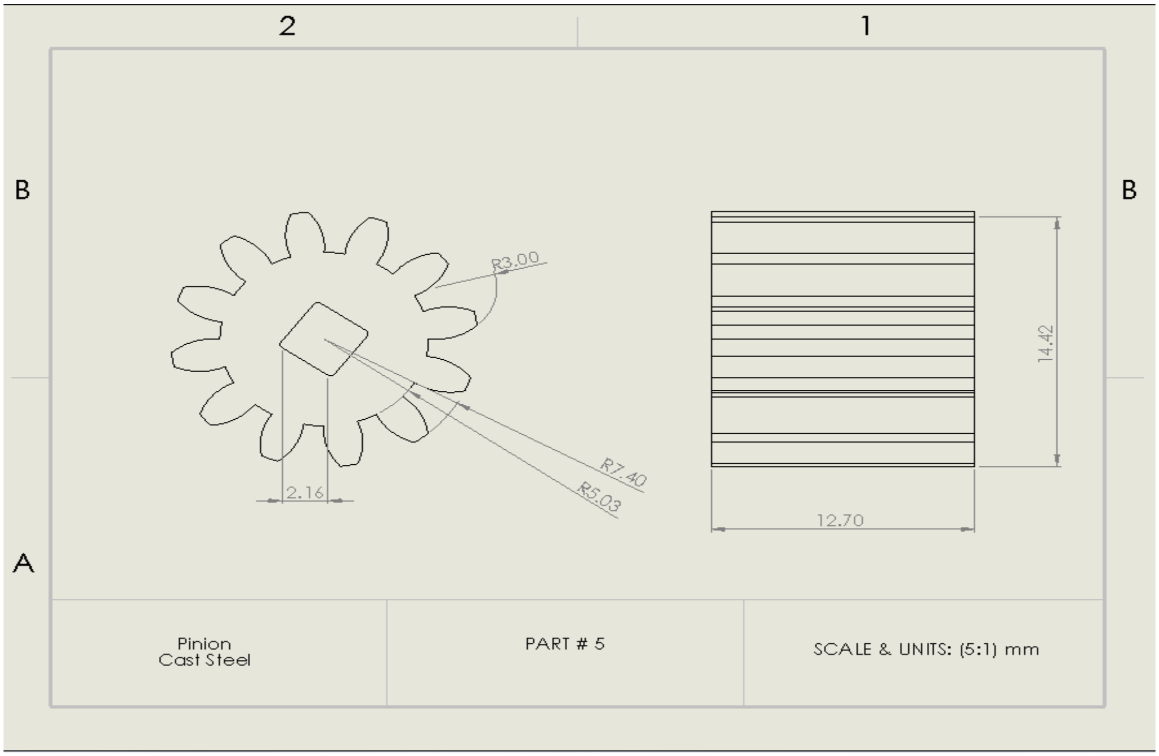

Pinion Cast Steel	PART # 5	SCALE & UNITS: (5:1) mm

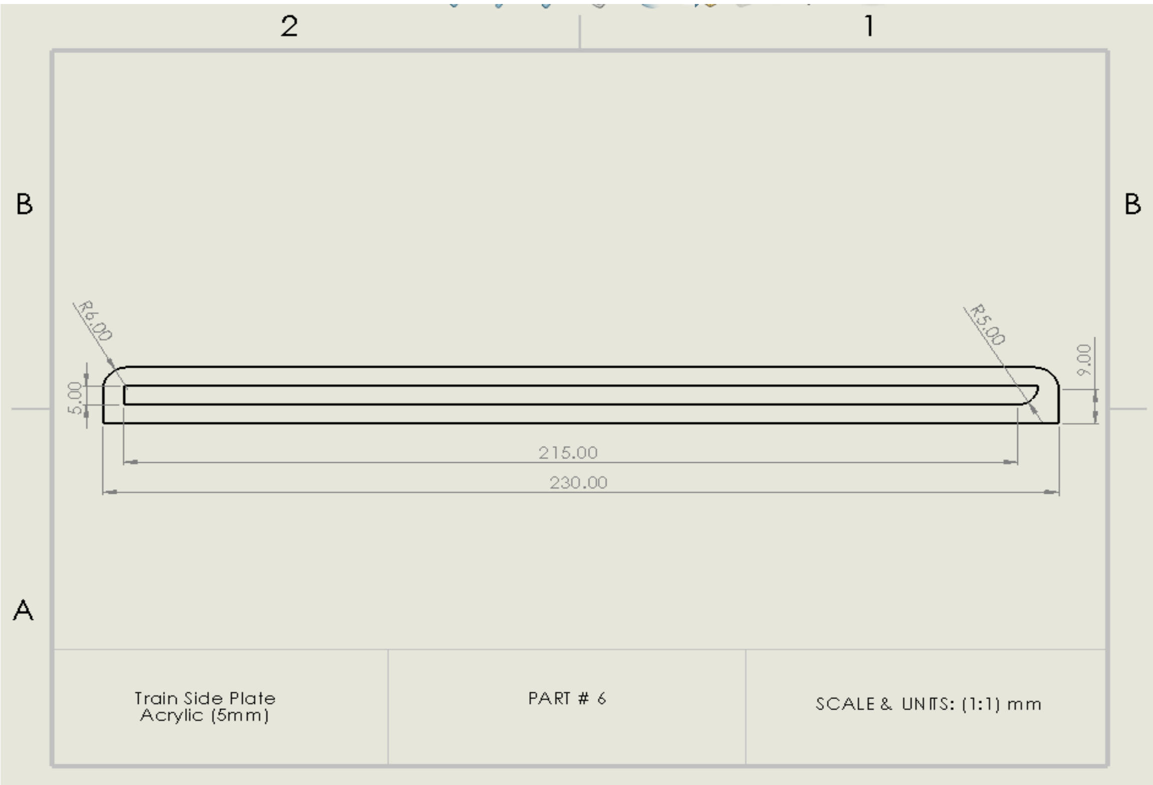

Train Side Plate Acrylic (5mm)	PART # 6	SCALE & UNITS: (1:1) mm

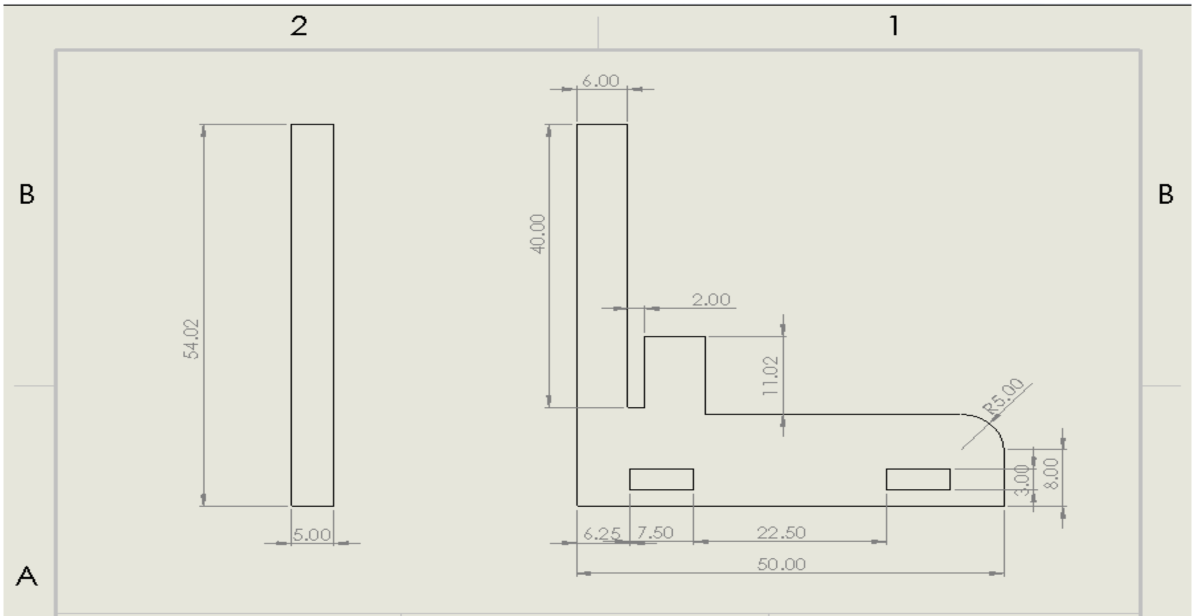

Train Slider Acrylic (5mm)	PART # 7	SCALE & UNITS: (2:1) mm

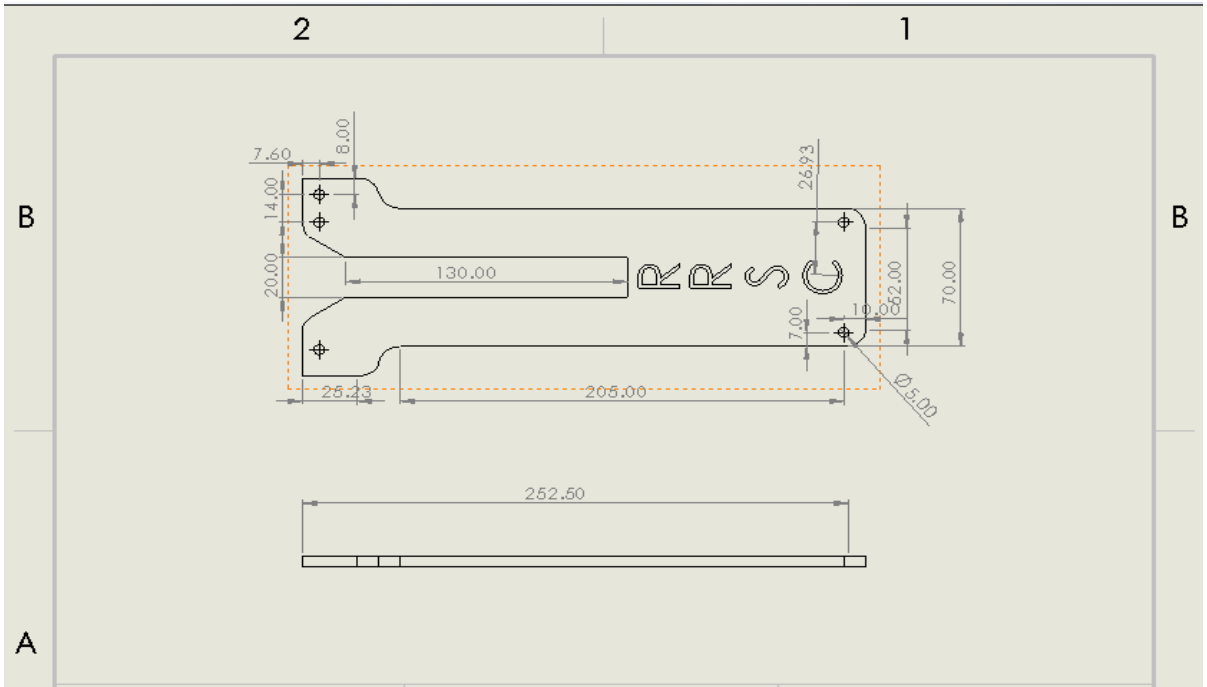

Train Base Acrylic (5mm)	PART # 8	SCALE & UNITS: (1:2) mm

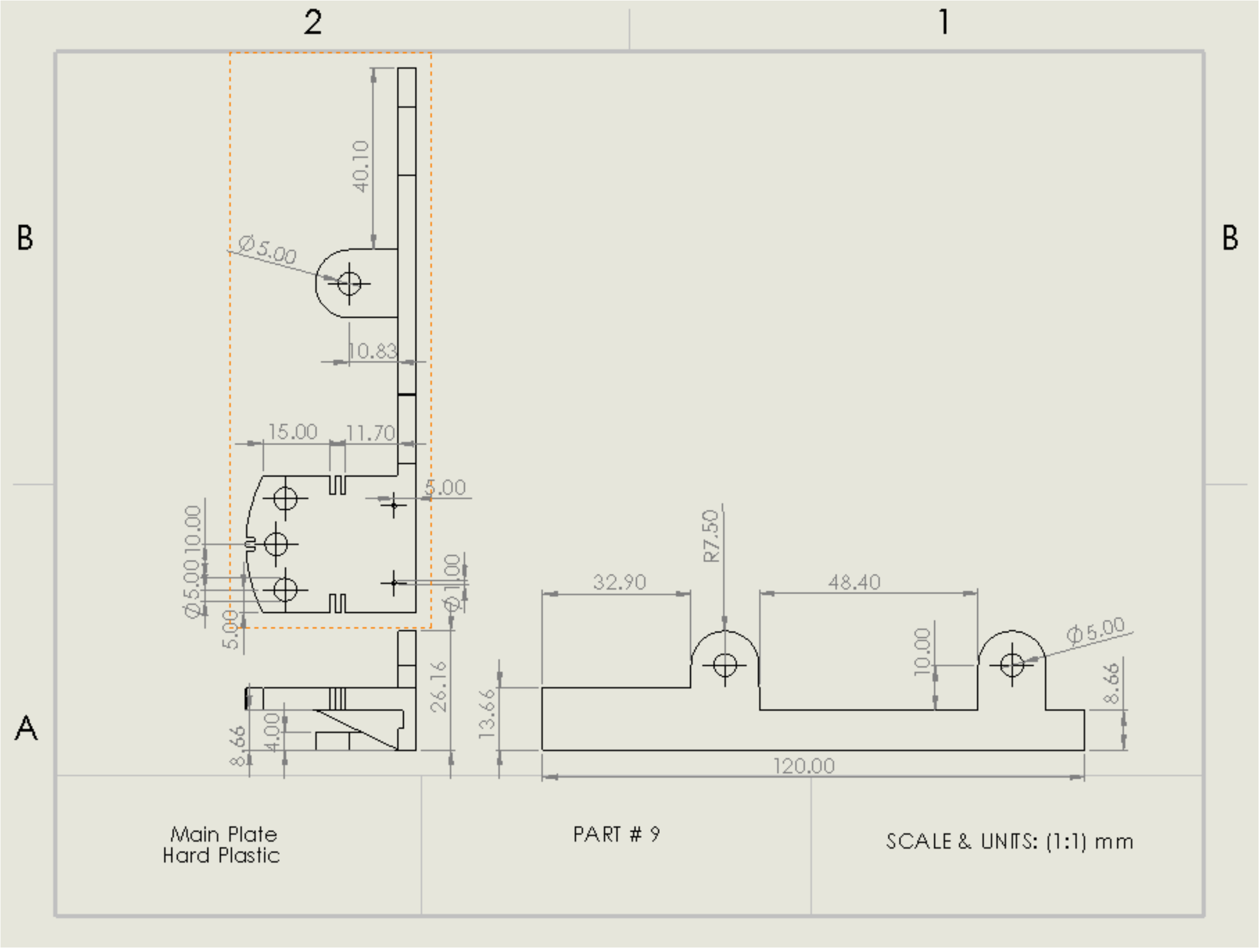

Main Plate
Hard Plastic

PART # 9

SCALE & UNITS: (1:1) mm

9.3 Appendix 3: Calibration Data from Milestone 2

Table 6: Static Calibration & Error Results.

	Volts	%FSO
Sensitivity	±0.12 V/cm	±7.67%
Non-linearity	±0.47	±31.33%
Zero Offset	±0.47	±31.33%
Repeatability	±0.25	±16.33%
Hysteresis	±0.19	±12.33%
FSO	3V	-

Table 7: Dynamic Calibration Results

	Time
Settling time	20 ms
Rise time	1.8 μs

9.4 Appendix 4: Final Calibration Data

Table 8: Final Calibration Data

Distance from Sensor (cm)	Cycle 1 (V)	Cycle 2 (V)	Average (V)
11	1.09	1.09	1.09
10	1	0.99	0.995
9	0.93	0.93	0.93
8	0.86	0.86	0.86
7	0.81	0.81	0.81
6	0.76	0.75	0.755
5	0.71	0.71	0.71
4	0.66	0.67	0.665
8	0.62	0.63	0.625
2	0.59	0.59	0.59
1	0.55	0.55	0.55
0	0.53	0.53	0.53
0	0.53	0.53	0.53
1	0.55	0.55	0.55
2	0.58	0.58	0.58
3	0.62	0.62	0.62
4	0.66	0.67	0.665
5	0.71	0.71	0.71
6	0.74	0.75	0.745
7	0.81	0.8	0.805
8	0.86	0.86	0.86
9	0.92	0.93	0.925
10	1.01	0.99	1
11	1.09	1.09	1.09

9.5 Appendix 5: Static Error Calculation

Table 9: Static Error Calculations

Voltage (V)	Deviation (Cycle 1)	Deviation (Cycle 2)	Dev 1 - Dev 2	Hysteresis (Cycle 1)	Hysteresis (Cycle 2)
1.096	0.006	0.006	0	0	0
0.997	-0.003	0.007	-0.01	-0.01	0
0.923	-0.007	-0.007	0	0.01	0
0.86	0	0	0	0	0
0.805	-0.005	-0.005	0	0	0.01
0.756	-0.004	0.006	-0.01	0.02	0
0.71	0	0	0	0	0
0.668	0.008	-0.002	0.01	0	0
0.629	0.009	-0.001	0.01	0	0.01
0.591	0.001	0.001	0	0.01	0.01
0.555	0.005	0.005	0	0	0
0.521	-0.009	-0.009	0	0	0